

Sensitivity analysis for the design of profile extrusion dies

J. Sienz^{a,*}, A. Goublomme^b, M. Luege^a

^aSwansea University, Centre for Polymer Processing Simulation and Design, School of Engineering, Swansea, Wales, UK

^bFluent Benelux, Avenue Pasteur 4, 1300 Wavre, Belgium

ARTICLE INFO

Article history:

Received 23 April 2009

Accepted 2 February 2010

Available online 9 March 2010

Keywords:

Sensitivity analysis

Shape optimization

Polymer processing

Extrusion die design

Finite element method

ABSTRACT

This paper proposes a procedure for design sensitivity analysis using the direct differentiation method which can be easily included into a finite element code. By a reformulation of the governing equations, it is shown that the derivatives necessary to evaluate the sensitivity of a given performance measure corresponding to the current design configuration can be obtained through a post-processing step by the same finite element solver used to solve the discrete state equations. The procedure is illustrated for some examples with known analytical expression of the sensitivity and then applied to several practical problems in the design of an extrusion process.

© 2010 Elsevier Ltd. All rights reserved.

1. Introduction

Extrusion is the process used to manufacture products in the form of continuous lengths with a uniform cross section. It is the task of the die to convert the cylindrical flow from the extruder into the required cross section. The design of a profile die is consequently a formidable task due to the intricate cross sections and tight dimensional tolerances that are usually required, coupled with the complexity of the flow phenomena involved in extrusion.

The significant advances of the modelling techniques during the recent years have made possible the simulation of the complex physical phenomena occurring in manufacturing processes. By now, there are several commercial and research software tools that have been developed for these simulations [1]. By including in such codes also the facility of the design sensitivity analysis, one can obtain an efficient design methodology.

A sensitivity analysis, which is the subject of the current paper, aims to quantitatively estimate the importance of a given change of parameters or design variables with respect to a global die design, without requiring trial and error attempts. It also represents a step in gradient-based optimization algorithms [2–5].

Progress in sensitivity analysis described for instance in [5–9], have made it feasible to use intensive numerical methods in design optimization for real applications in general [10,11,3] and in material processing designs such as polymer extrusion [10,12–14], metal forming processes [15], die shape design in sheet metal

stamping processes [7], and polymer injection and compression moulding processes [12,16], in particular.

In mathematical terms, the objective of a sensitivity analysis is the evaluation of the derivative of a given performance measure with respect to the design variables for given admissible configurations. The performance measure quantifies a certain process behaviour that one means to monitor. It is generally expressed as functional of the design variables and of the response or state variables. Since the state variables generally depend on the design variables through the state or equilibrium equations, the main concern in the sensitivity analysis is the evaluation of the implicit variations of these variables. The most common and used methods that are found in the literature are [6,17]: the finite difference method (FDM); the adjoint variable method (AVM); and the direct differentiation method (DDM). FDM represents the most straightforward way to compute sensitivities: a small design perturbation is introduced for each design variables, and the gradient of the response is then computed using a finite difference scheme to approximate the derivative. FDM is easy to implement although computationally expensive, since it requires that the problem is solved again for the perturbed value of each of the design variable. This method will however be considered in this paper to assess the proposed procedure. The AVM uses the solution to the adjoint problem to eliminate the implicit derivations that appear in the performance measure; its use is convenient when there are many performance measures to be considered. However, for the case of nonlinear problems, the AVM applies to a linearization version. DDM uses implicit differentiation to differentiate the state variables, involving the differentiation of the governing equations, and can be applied also to nonlinear problems.

* Corresponding author.

E-mail address: j.sienz@swansea.ac.uk (J. Sienz).

An important aspect in the design problem of an extrusion process concerns the geometry change. In such a case the governing equation will be defined in a variable domain, and therefore parameters that control the geometry of the body need to be included in the set of design variables. The domain parameterization method [18,19] and the material derivative method [20–22] are alternative techniques to represent the shape variations. The former method defines the derivatives assuming a fixed reference domain and applies the chain rule. A transformation that links the fixed reference domain, i.e. an invariant geometry, with the material coordinates is also inherent to FEM implementation where element coordinates serve as reference coordinates and the shape design variation can be represented by variations of the nodal coordinates, with the shape functions held fixed [17,23]. The material derivative method defines the derivatives at the undeformed (or initial) configuration instead, and depends on the domain design velocity, which represents the direction of a given design perturbation.

In this paper we are concerned with the inclusion of a sensitivity analysis approach into a finite element (FE) code using the DDM. Unlike current methods for sensitivity analysis and in order to keep the modifications to the FE code at a minimum, we develop a single procedure that yields the solution, the sensitivity values and the performance measure values within the same iterative strategy employed to solve the governing system of equations. The details of the sensitivity formulations are fully consistent with the details of the numerical model and the solution algorithm used in the simulation. This means that identical spatial discretization, interpolation functions and degrees of freedom are considered in the simulation and the design derivatives of the state variables are all well defined [17]. Highly accurate sensitivity predictions can therefore be obtained with the proposed procedure. The striking feature of our procedure is that it can be easily implemented in existing finite element codes without changes to the core part of the codes, i.e. the solver and the data structure.

With the aim of providing a powerful, flexible design aid for interactive use by the designer, the proposed sensitivity analysis approach is implemented into the commercial, finite element POLYFLOW [24] solver and included into an extrusion die design environment. This design environment is based on the classic three-column concept [25] and consists of: the structural model; the optimization algorithm, and the (design) optimization model.

The remainder of the paper is organized as follows: in Section 2 we introduce a consistent sensitivity analysis formulation for a steady state problem, formulated for treating the case of change of shapes using the domain parameterization method. In Section 3 we propose a numerical procedure to evaluate the sensitivity of a performance measure for any given design configuration within the same iterative strategy used to solve the governing system of equations. The proposed procedure is then developed in full details for two classical analytical examples in Section 4 with the expressions of the augmented matrices given in the Appendix. The procedure is then applied to the design of extrusion dies in Section 5. In Section 6 we validate the procedure by applying it to the design of two industrial dies. This is followed by the conclusions in Section 7.

2. Sensitivity analysis

This section introduces the design sensitivity analysis for the steady state response of a discrete system obtained by applying the FE method. We denote by $\mathbf{b}^T = [b^1, \dots, b^k] \in R^k$ the vector of design or control variables. The vector \mathbf{b} can include shape and/or non-geometric variables, such as material properties. The domain parameterization method is used to represent the design geometry [18], and the direct differentiation method is adopted to evaluate the derivative of the implicitly defined variables.

2.1. Statement of the problem

Let us denote by $F: R^k \times R^{m \times d} \times R^{m \times d} \rightarrow R$ a scalar function which represents a *performance measure*, such as, weight of the structure, displacement at a point, mean stress in a certain region, pressure drop across a die, exit velocities, and define

$$f(\mathbf{b}) := F(\mathbf{b}, \mathbf{x}(\mathbf{b}), \mathbf{u}(\mathbf{b})) \quad (1)$$

with $\mathbf{x} \in R^{m \times d}$ for $m = 1, 2, 3$ denoting the nodal coordinates of the FE mesh, d the number of nodes, and $\mathbf{u} \in R^{m \times d}$ the discrete solution of the state equation. We assume that for a given \mathbf{b} , there exists a mapping $\mathbf{R}_X: R^k \times R^{m \times d} \rightarrow R^{m \times d}$ such that \mathbf{x} is defined implicitly in terms of \mathbf{b} by the following equation

$$\mathbf{R}_X(\mathbf{b}, \mathbf{x}(\mathbf{b})) = 0 \quad (2)$$

Also, the mapping $\mathbf{R}_U: R^k \times R^{m \times d} \times R^{m \times d} \rightarrow R^{m \times d}$ is introduced to represent the discrete form of the state equations as follows

$$\mathbf{R}_U(\mathbf{b}, \mathbf{x}(\mathbf{b}), \mathbf{u}(\mathbf{b})) = 0 \quad (3)$$

2.2. Design sensitivity analysis

The sensitivity analysis aims to quantify the change in value of the assigned performance measure for a given variation of the design variable. This amounts to compute the derivative of f with respect to \mathbf{b} . Assuming that F , together with \mathbf{R}_X and \mathbf{R}_U , enjoy all the regularity properties we need, and using the chain rule we have

$$\frac{df}{d\mathbf{b}} = \frac{\partial F}{\partial \mathbf{b}} + \frac{\partial F}{\partial \mathbf{x}} \frac{\partial \mathbf{x}}{\partial \mathbf{b}} + \frac{\partial F}{\partial \mathbf{u}} \frac{\partial \mathbf{u}}{\partial \mathbf{b}} \quad (4)$$

In Eq. (4), the derivatives $\frac{\partial F}{\partial \mathbf{b}}$, $\frac{\partial F}{\partial \mathbf{x}}$ and $\frac{\partial F}{\partial \mathbf{u}}$ can in general easily be evaluated, given the explicit dependence of F on \mathbf{x} , \mathbf{u} and \mathbf{b} ; whereas the evaluation of $\frac{\partial \mathbf{x}}{\partial \mathbf{b}}$ and $\frac{\partial \mathbf{u}}{\partial \mathbf{b}}$ offers major difficulties since the variables \mathbf{x} and \mathbf{u} are implicit functions of \mathbf{b} . Differentiating Eqs. (2) and (3) yields

$$\begin{aligned} \frac{d\mathbf{R}_X}{d\mathbf{b}} = 0 &= \frac{\partial \mathbf{R}_X}{\partial \mathbf{b}} + \frac{\partial \mathbf{R}_X}{\partial \mathbf{x}} \frac{\partial \mathbf{x}}{\partial \mathbf{b}} \\ \frac{d\mathbf{R}_U}{d\mathbf{b}} = 0 &= \frac{\partial \mathbf{R}_U}{\partial \mathbf{b}} + \frac{\partial \mathbf{R}_U}{\partial \mathbf{x}} \frac{\partial \mathbf{x}}{\partial \mathbf{b}} + \frac{\partial \mathbf{R}_U}{\partial \mathbf{u}} \frac{\partial \mathbf{u}}{\partial \mathbf{b}} \end{aligned} \quad (5)$$

that can be rewritten as follows:

$$\begin{aligned} \frac{\partial \mathbf{R}_X}{\partial \mathbf{x}} \frac{\partial \mathbf{x}}{\partial \mathbf{b}} &= -\frac{\partial \mathbf{R}_X}{\partial \mathbf{b}}, \\ \frac{\partial \mathbf{R}_U}{\partial \mathbf{u}} \frac{\partial \mathbf{u}}{\partial \mathbf{b}} &= -\left(\frac{\partial \mathbf{R}_U}{\partial \mathbf{b}} + \frac{\partial \mathbf{R}_U}{\partial \mathbf{x}} \frac{\partial \mathbf{x}}{\partial \mathbf{b}} \right) \end{aligned} \quad (6)$$

and must be solved with respect to the components of the matrices $\frac{\partial \mathbf{x}}{\partial \mathbf{b}}$ and $\frac{\partial \mathbf{u}}{\partial \mathbf{b}}$.

Remark. Notice that $\frac{\partial \mathbf{R}_U}{\partial \mathbf{u}}$ is a matrix $(m \times d) \times (m \times d)$ and $\frac{\partial \mathbf{u}}{\partial \mathbf{b}}$ is a matrix $(m \times d) \times k$, hence $\frac{\partial \mathbf{R}_U}{\partial \mathbf{u}} \frac{\partial \mathbf{u}}{\partial \mathbf{b}}$ denotes the standard row by column product between matrices. The same observation applies for the other terms.

3. Numerical procedure

In this section we show that for any given design configuration the sensitivity of f can be evaluated within the same iterative strategy used to solve the nonlinear equations (2) and (3). Let $\bar{\mathbf{b}}$ denote the value of the design variables defining the given configuration, then Eqs. (1)–(3) can be equivalently written as follows:

Find $[\mathbf{b}, \mathbf{x}, \mathbf{u}, f]$ such that :

$$\begin{aligned} \mathbf{R}_b(\mathbf{b}) &:= \mathbf{b} - \bar{\mathbf{b}} = \mathbf{0} \\ \mathbf{R}_X(\mathbf{b}, \mathbf{x}) &= \mathbf{0} \\ \mathbf{R}_U(\mathbf{b}, \mathbf{x}, \mathbf{u}) &= \mathbf{0} \\ R_F(\mathbf{b}, \mathbf{x}, \mathbf{u}, f) &:= f - F(\mathbf{b}, \mathbf{x}, \mathbf{u}) = 0 \end{aligned} \quad (7)$$

For a given $\bar{\mathbf{b}}$, Eq. (7)₁ simply states $\mathbf{b} = \bar{\mathbf{b}}$, hence, Eq. (7)₂ and Eq. (7)₃ define \mathbf{x} and \mathbf{u} as solution of Eqs. (2) and (3) for $\mathbf{b} = \bar{\mathbf{b}}$, whereas Eq. (7)₄ yields the corresponding value of the performance measure.

By introducing the notation $\mathbf{R}^T := [\mathbf{R}_b, \mathbf{R}_x, \mathbf{R}_u, \mathbf{R}_f]$ and $\mathbf{P}^T := [\mathbf{b}, \mathbf{x}, \mathbf{u}, f]$, Eq. (7) can be written in a compact form as follows

$$\text{Find } \mathbf{P}, \text{ such that :} \quad \mathbf{R}(\mathbf{P}) = \mathbf{0} \quad (8)$$

By solving Eq. (8) with the Newton–Raphson method, one is led to consider the following iteration until convergence is reached:

$$\text{Given } \mathbf{P}^k, \text{ find } \mathbf{P}^{k+1} \text{ such that} \quad \mathbf{R}(\mathbf{P}^k) + \left. \frac{d\mathbf{R}}{d\mathbf{P}} \right|_{\mathbf{P}^k} (\mathbf{P}^{k+1} - \mathbf{P}^k) = \mathbf{0} \quad (9)$$

where $\mathbf{P}^{k+1} = [\mathbf{b}^k + \Delta\mathbf{b}, \mathbf{x}^k + \Delta\mathbf{x}, \mathbf{u}^k + \Delta\mathbf{u}, f^k + \Delta f]$. In matrix form Eq. (9) reads as

$$\begin{bmatrix} \frac{\partial \mathbf{R}_b}{\partial \mathbf{b}} & \mathbf{0} & \mathbf{0} & \mathbf{0} \\ \frac{\partial \mathbf{R}_x}{\partial \mathbf{b}} & \frac{\partial \mathbf{R}_x}{\partial \mathbf{x}} & \mathbf{0} & \mathbf{0} \\ \frac{\partial \mathbf{R}_u}{\partial \mathbf{b}} & \frac{\partial \mathbf{R}_u}{\partial \mathbf{x}} & \frac{\partial \mathbf{R}_u}{\partial \mathbf{u}} & \mathbf{0} \\ \frac{\partial \mathbf{R}_f}{\partial \mathbf{b}} & \frac{\partial \mathbf{R}_f}{\partial \mathbf{x}} & \frac{\partial \mathbf{R}_f}{\partial \mathbf{u}} & \frac{\partial \mathbf{R}_f}{\partial f} \end{bmatrix}^k \begin{bmatrix} \Delta \mathbf{b} \\ \Delta \mathbf{x} \\ \Delta \mathbf{u} \\ \Delta f \end{bmatrix} = \begin{bmatrix} -\mathbf{R}_b \\ -\mathbf{R}_x \\ -\mathbf{R}_u \\ -\mathbf{R}_f \end{bmatrix}^k \quad (10)$$

Since the solution of Eq. (7) defines \mathbf{x} , \mathbf{u} and f as implicit function of \mathbf{b} , from (8) it follows that $\frac{d\mathbf{R}}{d\mathbf{b}} = \mathbf{0}$. Using the chain rule we can therefore write

$$\frac{d\mathbf{R}}{d\mathbf{b}} = \frac{\partial \mathbf{R}}{\partial \mathbf{b}} + \frac{\partial \mathbf{R}}{\partial \mathbf{x}} \frac{d\mathbf{x}}{d\mathbf{b}} + \frac{\partial \mathbf{R}}{\partial \mathbf{u}} \frac{d\mathbf{u}}{d\mathbf{b}} + \frac{\partial \mathbf{R}}{\partial f} \frac{df}{d\mathbf{b}} = \mathbf{0} \quad (11)$$

which in matrix form reads as

$$\begin{bmatrix} \frac{\partial \mathbf{R}_b}{\partial \mathbf{b}} & \mathbf{0} & \mathbf{0} & \mathbf{0} \\ \frac{\partial \mathbf{R}_x}{\partial \mathbf{b}} & \frac{\partial \mathbf{R}_x}{\partial \mathbf{x}} & \mathbf{0} & \mathbf{0} \\ \frac{\partial \mathbf{R}_u}{\partial \mathbf{b}} & \frac{\partial \mathbf{R}_u}{\partial \mathbf{x}} & \frac{\partial \mathbf{R}_u}{\partial \mathbf{u}} & \mathbf{0} \\ \frac{\partial \mathbf{R}_f}{\partial \mathbf{b}} & \frac{\partial \mathbf{R}_f}{\partial \mathbf{x}} & \frac{\partial \mathbf{R}_f}{\partial \mathbf{u}} & \frac{\partial \mathbf{R}_f}{\partial f} \end{bmatrix} \begin{bmatrix} \frac{d\mathbf{b}}{d\mathbf{b}} \\ \frac{d\mathbf{x}}{d\mathbf{b}} \\ \frac{d\mathbf{u}}{d\mathbf{b}} \\ \frac{df}{d\mathbf{b}} \end{bmatrix} = \begin{bmatrix} \mathbf{0} \\ \mathbf{0} \\ \mathbf{0} \\ \mathbf{0} \end{bmatrix} \quad (12)$$

Noting that the matrix in Eq. (12) is the same as in Eq. (10), once the Newton–Raphson iteration has converged, we can also obtain the derivatives in Eq. (4) required to compute the sensitivity of f by simply performing a back substitution in Eq. (12).

It is also worth noting that, for the solver, there is no real distinction between the objective functions and the constraint functions as both functions are defined implicitly. This will be clearer later in the analytical examples.

The optimization of the design of an extrusion die is realized within the so called *extrusion die design environment* which consists of the following main components: (i) a *CFD solver* (POLYFLOW [24,31]) for computing the flow response together with the objective and constraint functions evaluation and computation of their respective sensitivities, (ii) an *optimization package* (DOT [26]) using a sequential quadratic programming method for optimizing the die design, and (iii) an *optimization scheme* (POLYOPT [27]) to control the overall process and provide the necessary data interfaces. The interaction between the individual components is shown in Fig. 1.

The new procedure appears to be a powerful tool to calculate the sensitivities by simply enlarging the system of equations that is sent to the solver. The commercial solver has been therefore augmented to compute function values for the objective and the constraints as well as their sensitivities. The application of this design tool is used throughout the example sections demonstrating the validity of the approach for a wide range of different problems.

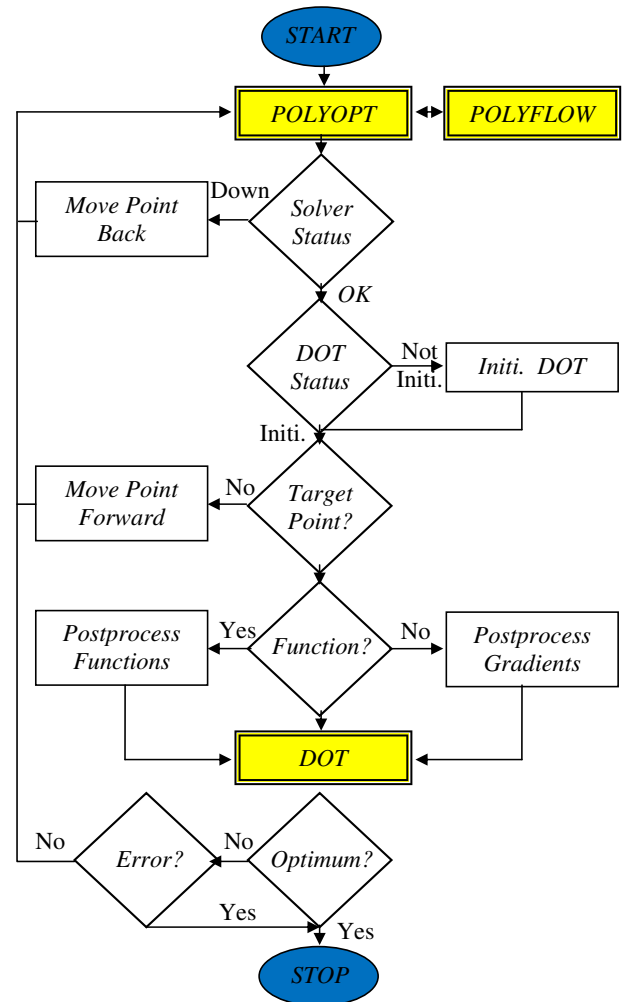


Fig. 1. Flow chart including POLYOPT, POLYFLOW and DOT.

4. Analytical examples

This section presents the application of the proposed procedure to some classical problems for which it is possible to analytically compute the sensitivity of the given performance measure. This is done to detail and visualize the steps needed to create the augmented matrices for the solution of the discrete state equations and the sensitivity analysis as a combined problem. The procedure is therefore developed in the following **Problem 1**, whereas **Problems 2 and 3** address different aspects to the actual implementation of the procedure.

4.1. 1D elastic bar problem

The bar of Fig. 2, fixed at both ends, with length L , and stiffness K , subjected to a uniform load equal to one, is used to illustrate the proposed procedure for the case of two design variables with $\mathbf{b} = \{L, K\}$. The objective is to find the values for the design variables to satisfy

$$u\left(\frac{L}{2}\right) = 1 \quad (13)$$

Problem 1. 1D elastic bar problem with two design variables $\mathbf{b} = \{L, K\}$.

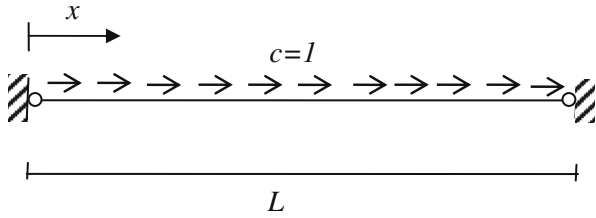


Fig. 2. Model problem.

4.1.1. Continuum model

The equilibrium of the elastic bar shown in Fig. 2 is governed by the state equation

$$K \frac{d^2 u}{dx^2} + 1 = 0 \quad x \in]0, L[$$

$$u(0) = u(L) = 0 \tag{14}$$

with the analytical solution

$$u(x) = \frac{Lx - x^2}{2K} \tag{15}$$

Assuming the following performance measure

$$F(L, u) = \left(u\left(\frac{L}{2}\right) - 1 \right)^2 \tag{16}$$

a function of L and K , we introduce a constraint equation as

$$g(L) = L - 2 \leq 0 \tag{17}$$

Note that the design variables, $\mathbf{b} = \{L, K\}$, are of different type, i.e. of geometric and material type, respectively. The governing equation will therefore be written in a reference configuration using the domain parameterization method [17,19]. The application of this method is quite natural when using the FE method, if referring to the isoparametric formulation of the finite elements. The local coordinates of each element can be indeed taken as the reference coordinate system.

4.1.2. FE model

By introducing on $\Omega = [0, L]$, a finite element mesh of N linear bar elements (see Fig. 3) and equally spaced nodes i , for $i = 1, \dots, N + 1$, the nodal coordinates x_i are given by

$$x_i = \frac{i - 1}{N} L \tag{18}$$

whereas the state variable $\mathbf{u} = [u_1, \dots, u_{N+1}]$, representing the axial displacement of the nodes, is obtained by solving the discrete equilibrium equation

$$\mathbf{R}_U = \mathbf{K}\mathbf{u} - \mathbf{C} = \mathbf{0} \tag{19}$$

with \mathbf{K} the global stiffness matrix, and \mathbf{C} the force vector, both dependent on the design variables L and K .

Assuming $N = 4$, for illustrative purposes, the discrete performance measure is given by

$$F(L, u) = (u_3 - 1)^2 \tag{20}$$

Recalling that in this 1D problem the FE solution u_i , $i = 1, \dots, N + 1$ coincides with the analytical solution at the nodes, we can explicitly

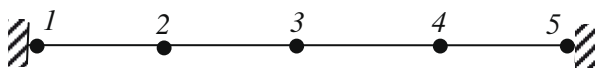


Fig. 3. FE model.

Table 1

Problem 1: position, displacement and sensitivities for each node i (analytical results).

Node i	1	2	3	4	5	
x_i	0	1/8	1/4	3/8	1/2	
u_i	0	3/256	1/64	3/256	0	
dx_i/dL	0	1/4	1/2	3/4	1	
du_i/dL	0	3/64	1/16	3/64	0	
du_i/dK	0	-3/512	-1/128	-3/512	0	
df_1/dL						-63/512
df_1/dK						63/4096

deduce the analytical expressions for the sensitivities of the performance measure and of the constraint, as follows

$$\frac{dF}{dL} = \frac{L}{2K} \left(\frac{L^2}{8K} - 1 \right), \quad \frac{dF}{dK} = -\frac{L^2}{2K^2} \left(\frac{L^2}{8K} - 1 \right) \tag{21}$$

$$\frac{dg}{dL} = 1, \quad \frac{dg}{dK} = 0$$

where the derivatives of \mathbf{u} and \mathbf{x} with respect to L are given by the following equations

$$\frac{dx_i}{dL} = \frac{i - 1}{N}, \quad \frac{du_i}{dL} = \frac{L}{K} \left(\frac{i - 1}{N} - \frac{(i - 1)^2}{N^2} \right) \tag{22}$$

The position, displacement and sensitivity values corresponding to $L = 0.5$ and $K = 2$ are reported in Table 1.

4.1.3. Numerical solution

For the given configuration $L = \bar{L}$ and $K = \bar{K}$, the solution of (18) and (19) can be obtained by solving the following system of equations

Given \bar{L} and \bar{K} , find $[L, K, \mathbf{x}, \mathbf{u}, f, g]$, such that :

$$R_L(L) = L - \bar{L} = 0$$

$$R_K(K) = K - \bar{K} = 0$$

$$R_{x_i}(L, \mathbf{x}) = x_i - \frac{i - 1}{N} L = 0 \quad \text{for } i = 1, \dots, 5$$

$$\mathbf{R}_U(L, K, \mathbf{x}, \mathbf{u}) = \mathbf{K}\mathbf{u} - \mathbf{C} = \mathbf{0} \tag{23}$$

$$R_F(L, K, \mathbf{x}, \mathbf{u}, f) = f - (u_3 - 1)^2 = 0$$

$$R_G(L, g) = g - L + 2 = 0$$

with the conditions :

$$u_1 = u_5 = 0$$

$$g \leq 0$$

In order to apply the Newton–Raphson method to Eq. (23), the following derivatives are needed

$$\frac{\partial R_L}{\partial L} = 1, \quad \frac{\partial R_K}{\partial K} = 1$$

$$\frac{\partial \mathbf{R}_X}{\partial \mathbf{x}} = 1; \quad \frac{\partial \mathbf{R}_X}{\partial \mathbf{b}} = \left\{ \frac{\partial \mathbf{R}_X}{\partial L} \quad \frac{\partial \mathbf{R}_X}{\partial K} \right\}$$

$$\frac{\partial \mathbf{R}_U}{\partial \mathbf{u}} = \mathbf{K}; \quad \frac{\partial \mathbf{R}_U}{\partial \mathbf{x}} = \frac{\partial \mathbf{K}}{\partial \mathbf{x}} \mathbf{u} - \mathbf{C}; \quad \frac{\partial \mathbf{R}_U}{\partial \mathbf{b}} = \left\{ \frac{\partial \mathbf{R}_U}{\partial L} \quad \frac{\partial \mathbf{R}_U}{\partial K} \right\} = \left\{ \mathbf{0} \quad \frac{1}{K} \mathbf{K} \right\}$$

$$\frac{\partial R_F}{\partial \mathbf{u}} = \{0 \quad -2(u_3 - 1) \quad 0\}; \quad \frac{\partial R_F}{\partial f} = 1;$$

$$\frac{\partial R_F}{\partial \mathbf{b}} = \left\{ \frac{\partial R_F}{\partial L} \quad \frac{\partial R_F}{\partial K} \right\} = \{0 \quad 0\}$$

$$\frac{\partial R_G}{\partial g} = 1; \quad \frac{\partial R_G}{\partial \mathbf{b}} = \left\{ \frac{\partial R_G}{\partial L} \quad \frac{\partial R_G}{\partial K} \right\} = \{-1 \quad 0\} \tag{24}$$

Further details on the expression of the partial derivatives (24)₃ can be found in Appendix. Since the boundary conditions are $u_1 = u_5 = 0$, the unknowns of this problem reduce to

Table 2

Problem 1: unknown nodal values obtained at each iteration.

Iteration	u_2	u_3	u_4	x_2	x_3	x_4	f	g	L	K
1st	3/128	1/32	3/128	1/8	1/4	3/8	15/16	-3/2	1/2	2
2nd	3/256	1/64	3/256	1/8	1/4	3/8	31/32	-3/2	1/2	2
3rd	3/256	1/64	3/256	1/8	1/4	3/8	3969/4096	-3/2	1/2	2

Table 3Problem 1: sensitivities with respect to L (numerical results).

$\partial_L u_2$	$\partial_L u_3$	$\partial_L u_4$	$\partial_L x_2$	$\partial_L x_3$	$\partial_L x_4$	$\partial_L f$	$\partial_L g$	$\partial_L L$	$\partial_L K$
3/64	1/16	3/64	1/4	1/2	3/4	-63/512	1	1	0

Table 4Problem 1: sensitivities with respect to K (numerical results).

$\partial_K u_2$	$\partial_K u_3$	$\partial_K u_4$	$\partial_K x_2$	$\partial_K x_3$	$\partial_K x_4$	$\partial_K f$	$\partial_K g$	$\partial_K L$	$\partial_K K$
-3/512	-1/128	-3/512	0	0	0	63/4096	0	0	1

$$\Delta \mathbf{u} = \begin{bmatrix} \Delta u_2 \\ \Delta u_3 \\ \Delta u_4 \end{bmatrix}; \quad \Delta \mathbf{x} = \begin{bmatrix} \Delta x_1 \\ \Delta x_2 \\ \Delta x_3 \\ \Delta x_4 \\ \Delta x_5 \end{bmatrix}; \quad \Delta f; \quad \Delta g; \quad \Delta \mathbf{b} = \begin{bmatrix} \Delta L \\ \Delta K \end{bmatrix} \quad (25)$$

For, $\bar{L} = 0.5$ and $\bar{K} = 2$, for instance, and the following initial conditions

$$\mathbf{u}^{k=0} = 0, \quad f^{k=0} = 0, \quad g^{k=0} = 0, \quad L^{k=0} = 1, \quad K^{k=0} = 2 \quad (26)$$

convergence of the iterative procedure has been achieved after three iterations as shown in Table 2. Tables 3 and 4 report the sensitivity with respect to the design variables L and K , respectively, which are equal to the analytical values reported in Table 1.

4.2. 1D heat conduction problem

The model problem is illustrated in Fig. 4. The state equations are the same as for the 1D elastic bar problem with the analytical solution given by Eq. (15), where K denotes now the conductivity and the state variable \mathbf{u} (displacement) is replaced by the temperature T . The objective is to find the values for the design variables so that the temperature in the centre of the domain satisfies

$$T\left(\frac{L}{2}\right) = 1 \quad (27)$$

Problem 2. 1D heat conduction with one design variable.

Assuming the performance measure as,

$$F(T, L) = \left(T\left(\frac{L}{2}\right) - 1\right)^2 = \left(\frac{L^2}{8K} - 1\right)^2 \quad (28)$$

for the derivative with respect to L we have

$$\frac{dF}{dL} = \frac{L}{2K} \left(\frac{L^2}{8K} - 1\right) \quad (29)$$

In this example we consider the additional side constraints on the design variable L given by

$$1 \leq L \leq 5 \quad (30)$$

which is convenient to express as

$$\begin{aligned} g_1(L) &= 1 - L \leq 0 \\ g_2(L) &= L - 5 \leq 0 \end{aligned} \quad (31)$$

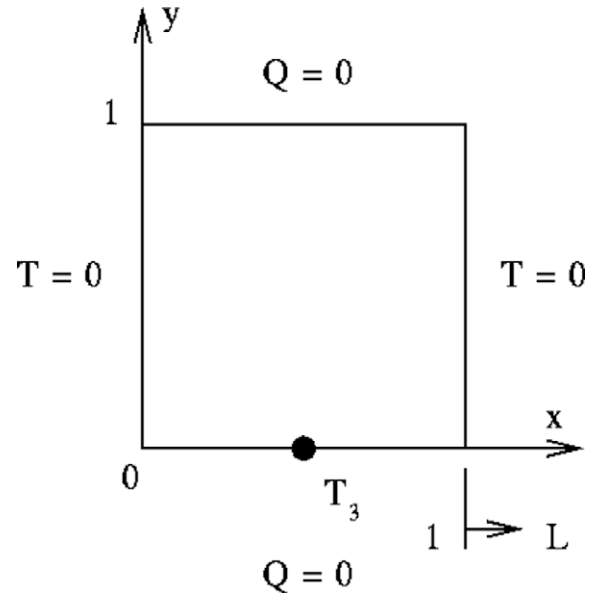


Fig. 4. Model problem for heat conduction along the x-axis.

Introducing the same FE mesh as in Problem 1, with $N = 4$, equally spaced nodes for illustrative purposes, the nodal coordinates are then given by Eq. (18), and the discretized state equation takes the form of Eq. (19) with $\mathbf{T}^T = [T_1, T_2, T_3, T_4, T_5]$.

The system of equations that defines the temperature distribution, in the configuration characterised by \bar{L} , is therefore the following

Given \bar{L} , find $[L, \mathbf{x}, \mathbf{u}, f, g_1, g_2]$, such that :

$$R_L(L) = L - \bar{L} = 0$$

$$R_{x_i}(L, \mathbf{x}) = x_i - \frac{i-1}{N}L = 0 \quad \text{with } i = 1, \dots, 5$$

$$\mathbf{R}_U(L, \mathbf{x}, \mathbf{T}) = \mathbf{KT} - \mathbf{C} = \mathbf{0}$$

$$R_f(L, \mathbf{x}, \mathbf{T}, f) = f - (T_3 - 1)^2 = 0$$

$$R_{g_1}(L, g_1) = g_1 - 1 + L = 0$$

$$R_{g_2}(L, g_2) = g_2 + 5 - L = 0$$

with the conditions :

$$T_1 = T_5 = 0$$

$$g_1 < 0$$

$$g_2 < 0$$

The system of Eq. (32) has been solved for different values of the design variable \bar{L} . The performance measure and its sensitivity have then been obtained: (i) analytically by evaluating the functions in Eq. (29); (ii) by the proposed procedure; and (iii) by using finite differences with a value of the perturbation $\Delta L = 0.0001$. Good agreement between the performance function and the sensitivity evaluated in the three different ways is observed by comparing the values displayed in Fig. 5. The finite difference evaluation of the sensitivity appears correct for up to three digits (see Table 5). This is due to the fact that the solver outputs the function values

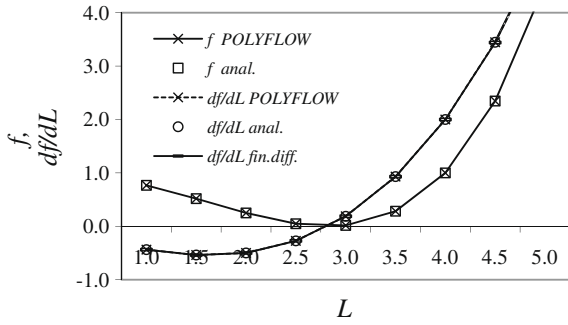


Fig. 5. Problem 2: values of the performance measure, f , and of its derivative with respect to L , df/dL , obtained analytically by the proposed procedure and by FDM.

Table 5
Problem 2: performance function value f and sensitivity value df/dL for different values of L , solved using the proposed procedure, analytically and FDM.

Length L	f	df/dL	f analytic	df/dL analytic	df/dL FDM
0.000	0.766	-0.438	0.766	-0.438	-0.438
0.500	0.517	-0.539	0.517	-0.539	-0.539
1.000	0.250	-0.500	0.250	-0.500	-0.500
1.500	0.048	-0.273	0.048	-0.273	-0.273
2.000	0.016	0.188	0.016	0.188	0.188
2.500	0.282	0.930	0.282	0.930	0.929
3.000	1.000	2.000	1.000	2.000	2.000
3.500	2.345	3.445	2.345	3.445	3.440
4.000	4.516	5.313	4.516	5.313	5.310

only with seven digits and the perturbation occurs in the fourth digit.

We also note that, graphically, the performance function attains a minimum which coincides with the analytical result at $L = \sqrt{8}$ where $df/dL = 0$.

After this design space study the automatic optimization was carried out. The convergence history for the optimization is displayed in Fig. 6 with full convergence achieved after four iterations and an optimal value of the performance function $F(L) = 0.7780^{-14}$.

Fig. 7 shows the FE mesh configurations for the initial design $L = 0$ and the final design $L = \sqrt{8}$.

Problem 3. 1D heat conduction with two design variables.

In this example, the design variables are now chosen to be the position of the extreme nodes. Assuming the same FE mesh of the previous examples, the performance measure is given by

$$F(x_1, x_5, \mathbf{T}) = (T_3 - 1)^2 = \left(\frac{(x_5 - x_1)^2}{8K} - 1 \right)^2 \tag{33}$$

with the constraints

$$\begin{aligned} x_1 &\leq 0.5 \\ 0.0 &\leq x_5 \leq 4.0 \\ x_5 - x_1 &> 0 \end{aligned} \tag{34}$$

where x_1 and x_5 are the end nodes coordinates. Since the FE solution T_i coincides with the analytical solution at x_i , the analytical expression of the sensitivity of the performance measure reads as

$$\frac{dF}{dx_1} = -\frac{dF}{dx_5} = -\frac{(x_5 - x_1)}{2K} \left(\frac{(x_5 - x_1)^2}{8K} - 1 \right) \tag{35}$$

from which follows that the gradient of F vanishes along the straight line with equation

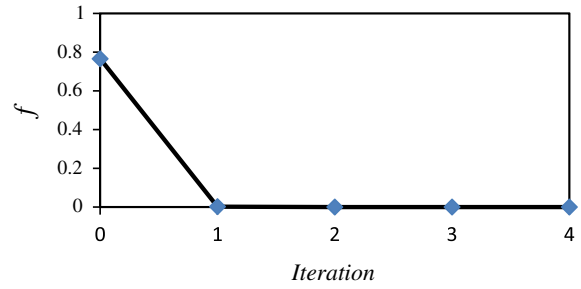


Fig. 6. Problem 2: convergence history for optimization.

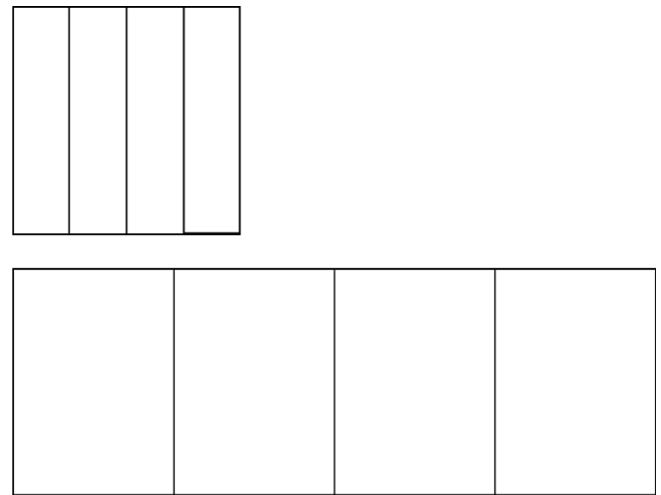


Fig. 7. Problem 2: initial design (top) ($L = 1.0$) and final design (bottom) ($L = 2.828$).

$$x_5 = x_1 + \sqrt{8} \tag{36}$$

The model problem is the same as in Fig. 4, where the FE discretization obtained for three different pairs of (\bar{x}_1, \bar{x}_5) , i.e. $(0.0, 1.0)$, $(0.5, 1.0)$ and $(-0.5, 4.0)$ is shown in Fig. 8. The system of equations that needs to be solved in this case can be therefore written as follows

Given \bar{x}_1, \bar{x}_5 , find $[\mathbf{x}, \mathbf{T}, f, \mathbf{g}]$, such that :

$$\begin{aligned} R_{x_1}(x_1) &= x_1 - \bar{x}_1 = 0 \\ R_{x_5}(x_5) &= x_5 - \bar{x}_5 = 0 \\ R_{x_i}(\mathbf{x}) &= x_i - \frac{i-1}{N}(x_5 - x_1) \quad \text{with } i = 2, 3, 4 \\ \mathbf{R}_U(\mathbf{x}, \mathbf{T}) &= \mathbf{KT} - \mathbf{C} = \mathbf{0} \\ R_F(\mathbf{x}, \mathbf{T}, f) &= f - (T_3 - 1)^2 = 0 \\ R_{g_1}(x_1, g_1) &= g_1 - x_1 + 0.5 = 0 \\ R_{g_2}(x_5, g_2) &= g_2 - x_5 + 4 = 0 \\ R_{g_4}(x_5, g_3) &= g_3 + x_5 = 0 \\ R_{g_4}(x_1, x_5, g_4) &= g_4 + x_5 - x_1 = 0 \end{aligned} \tag{37}$$

with the conditions :

$$\begin{aligned} T_1 = T_5 &= 0 \\ \mathbf{g} &\leq 0 \end{aligned}$$

where we have set $\mathbf{g} = [g_1, g_2, g_3, g_4]$ and the inequality $\mathbf{g} \leq 0$ is meant component-wise. Figs. 9 and 10 display the diagram of the analytical expression of the performance measure for the cases:

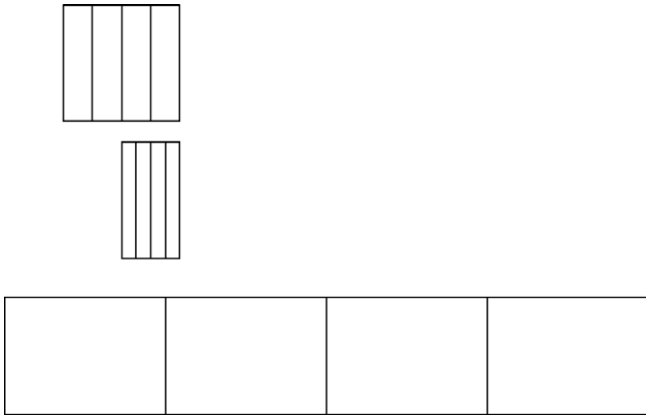


Fig. 8. Problem 3: FE models for: (a) $x_1 = 0.0$, $x_5 = 1.0$, (b) $x_1 = 0.5$, $x_5 = 1.0$ and (c) $x_1 = -0.5$, $x_5 = 4.0$.

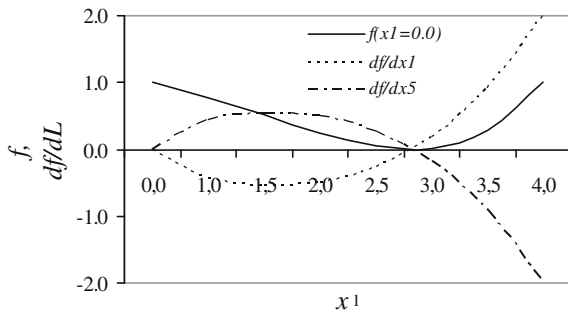


Fig. 9. Performance measure and sensitivity values for Problem 3 with $x_1 = 0.0$.

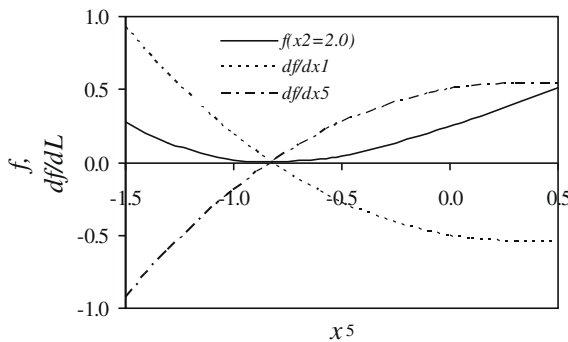


Fig. 10. Performance measure and sensitivity values for Problem 3 with $x_5 = 2.0$.

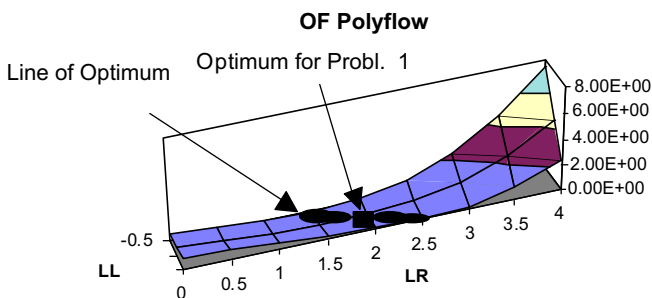


Fig. 11. Performance measure for Problem 3.

$x_1 = 0.0$, $x_5 \in [0.0, 4.0]$; and $x_1 \in [-1.5, 0.5]$, $x_5 = 2$, respectively. In the first case, f reaches a minimum at $x_1 = 0.0$, $x_5 = \sqrt{8}$ as shown in

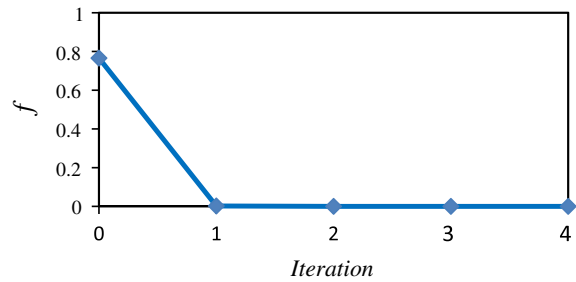


Fig. 12. Convergence history for optimization Problem 3.

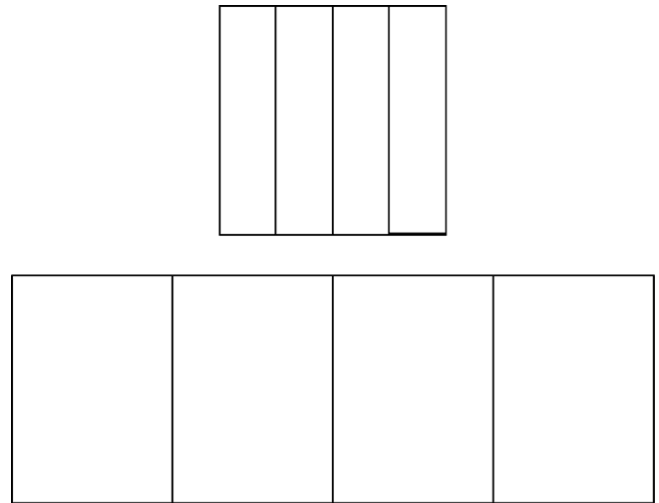


Fig. 13. Initial design (top) ($x_1 = 0$; $x_5 = 1.0$) and final design (bottom) ($x_1 = -0.91421$; $x_5 = 1.91421$) for Problem 3.

Fig. 9, whereas in the second case f reaches a minimum at $x_1 = 2.0 - \sqrt{8}$, $x_5 = 2.0$ (see Fig. 10).

The objective function is plotted in Fig. 11 for different values of the design variables x_1 and x_5 . Although the problem itself is straightforward we observe that the optimum is a line, hence each point on this line defined by a set of values for the two design variables will deliver the same optimum value. Therefore, there is no unique global solution. However, if the total length of the domain is chosen equal to $x_1 - x_5 = \sqrt{8}$, the minimizer will be unique.

The convergence history for the optimization is displayed in Fig. 12 showing also in this example, convergence after four iterations. The optimal value of the objective function is $F(x_1, x_2, 1) = 0.2832^{-14}$ which is achieved for the design variable values of $x_1 = -0.91421$; $x_5 = 1.91421$ after four new designs and fourteen full function evaluations. This result agrees well with the analytic solution. The temperature in the centre of the adjusted edge is equal to 1.0 within machine precision. The initial and the final designs are finally displayed in Fig. 13.

5. Sensitivity analysis for the design of an extrusion die

Extrusion is a manufacturing process used to obtain continuous profiles with a uniform cross section, which can be, for instance, circular, annular or rectangular [28]. A restriction zone or die land is placed perpendicular to the direction of the flow in order to force the polymer melt toward the die's outer edge. A major challenge in the extrusion process is the design of the die because of the deformation undergone by the flowing material right after the

die [29–32]. These deformations are mainly due to the combined effect of the velocity redistribution and the stress relaxation due to the viscoelasticity of the material.

Usually, the problems encountered in the die design can be one of the following two types:

- Exit flow uniformity or die balancing, which can be achieved by modifying of the up-stream part of the die.
- Free surface calculation with the objective of achieving the correct target cross-sectional area by modification of the die lips.

In the following, the latter type of design is addressed. Two die designs and one material design are analysed by considering different performance measures and/or design variables. These are:

- **Problem 4:** Design of the die length with pressure drop and average tangential velocity as performance measures;
- **Problem 5:** Design of the parallel section diameter with free surface height as performance measure;
- **Problem 6:** Material design with free surface height as performance measure.

Die designs based on exit flow uniformity are considered in Section 6 for applications in design optimization.

All melt flows are modelled by the Navier–Stokes equations which are solved numerically. The proposed procedure together with the evaluation of the sensitivity by FDM, have been implemented in this code.

Problem 4. Design of the die length with pressure drop and average tangential velocity as performance measures.

In this example, the die shown in Fig. 14 is designed to minimize the weighted sum of the average tangential velocity, \bar{v}_t , along the outlet plus the pressure drop, Δp , across the die by changing the length of the parallel section L at the die land. The pressure drop influences the extruder size and the power requirements, whereas the average tangential velocity can influence the final product homogeneity [13]. We therefore identify the following two performance measures,

$$F_1 = (\bar{v}_t)^2, \quad F_2 = (\Delta p)^2 \quad (38)$$

where $\Delta p = p_i - p_e$ and $\bar{v}_t = \frac{1}{d} \int_0^d v_t dz$, with v_t measured at the die land and d the height of the corresponding die section, in this case $d/2 = 1$. The functions given in Eq. (38) are used to define a single performance function f simply by associating with each F_i a weighting factor $w_i \geq 0$, with $\sum_{i=1}^k w_i = 1$, we set

$$f = w_1 \bar{F}_1 + w_2 \bar{F}_2 \quad (39)$$

where \bar{F}_i denotes the adimensional form of the functions in Eq. (38). Please note, this is to demonstrate the procedure. For industrial die

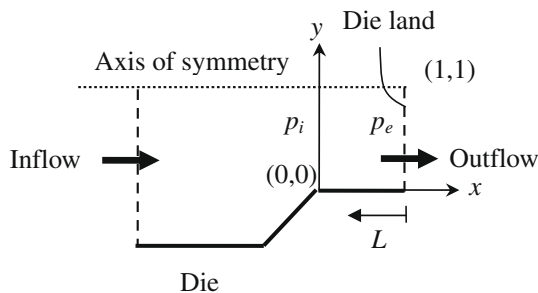


Fig. 14. Problem 4: model problem for an extrusion process with the length of the parallel zone L as design variable.

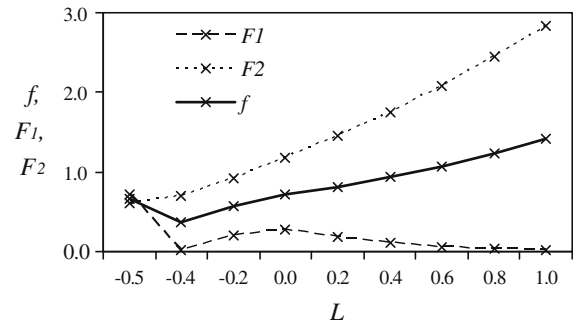


Fig. 15. Problem 4: performance values of F_1 , F_2 and f for different values of L obtained using results from POLYFLOW.

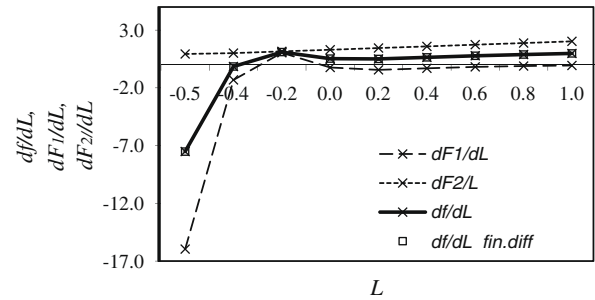


Fig. 16. Problem 4: sensitivity values $d\bar{F}_1/dL$, $d\bar{F}_2/dL$ and df/dL for different values of L obtained using the proposed procedure and the FDM.

Table 6

Problem 4: performance function values F_1 and F_2 and sensitivities dF_1/dL and dF_2/dL for different values of L , solved using the proposed procedure and FDM.

Length L	F_1	dF_1/dL	dF_1/dL FDM	F_2	dF_2/dL	dF_2/dL FDM
-0.500	0.179	-3.991	-3.994	6.11E+05	9.36E+05	9.36E+05
-0.400	0.004	-0.328	-0.329	7.08E+05	1.01E+06	1.01E+06
-0.200	0.052	0.259	0.259	9.25E+05	1.16E+06	1.16E+06
0.000	0.067	-0.059	-0.059	1.17E+06	1.30E+06	1.30E+06
0.200	0.047	-0.110	-0.110	1.45E+06	1.45E+06	1.45E+06
0.400	0.028	-0.077	-0.077	1.75E+06	1.59E+06	1.59E+06
0.600	0.016	-0.046	-0.046	2.08E+06	1.74E+06	1.73E+06
0.800	0.009	-0.027	-0.027	2.44E+06	1.88E+06	1.88E+06
1.000	0.004	-0.016	-0.016	2.83E+06	2.03E+06	2.02E+06

design, more elaborate multiobjective function tools should be used.

In this study, the flow length variation L , shown in Fig. 14, is taken as design variable subject to the following constraints:

$$-0.5 \leq L \leq 1.0 \quad (40)$$

where for $L = 0$ the die land is placed in its original position at $x = 1$.

The geometry of the die and boundary conditions are shown in Fig. 14. The melt flow across the die is modelled as a 2D problem and has been solved for different values of L .

Fig. 15 displays the variation of f , \bar{F}_1 and \bar{F}_2 with L for $w_2 = w_1 = 0.5$. As we can observe, the optimization problem is not very well posed, the average tangential velocity (\bar{F}_1) can be minimized by simply extending the length of the parallel section infinitely. The reduction in pressure drop (\bar{F}_2) demands the opposite, namely the shortening of the parallel section as much as possible. Furthermore, both parts of the performance function differ by a factor of six orders of magnitude in their values. A better posed problem would be obtained by minimizing the average tangential

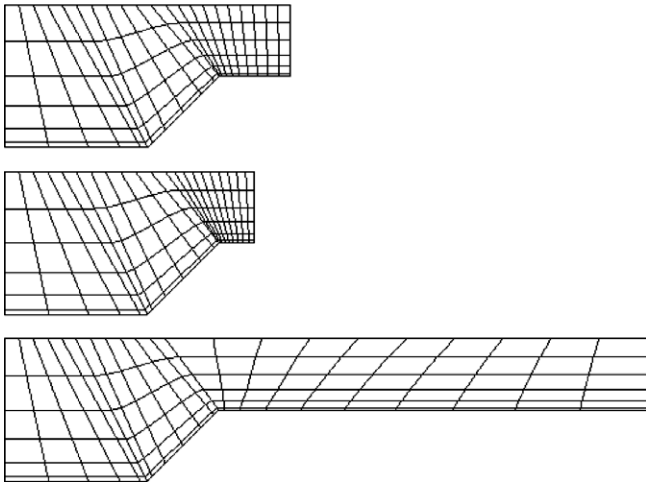


Fig. 17. Problem 4: FE discretization for different configurations: $L = 0.0$ (top), $L = -0.5$ (centre), and $L = 5.0$ (bottom).

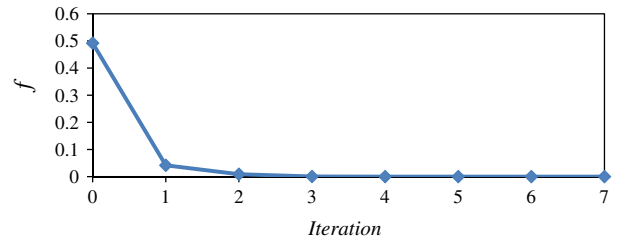


Fig. 21. Convergence history for Problem 5.

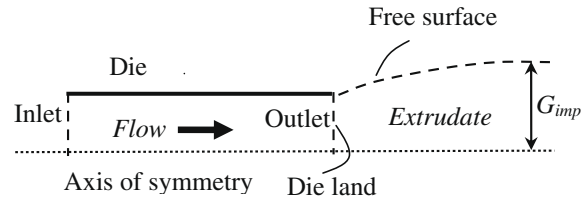


Fig. 22. Problem 6: die design with given final extrudate height G_{imp} .

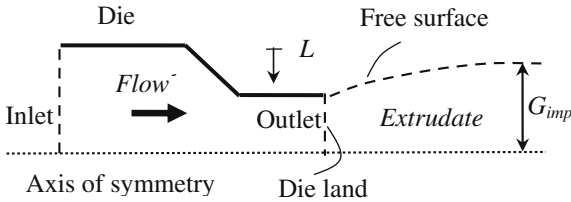


Fig. 18. Problem 5: die design with given final extrudate height G_{imp} .

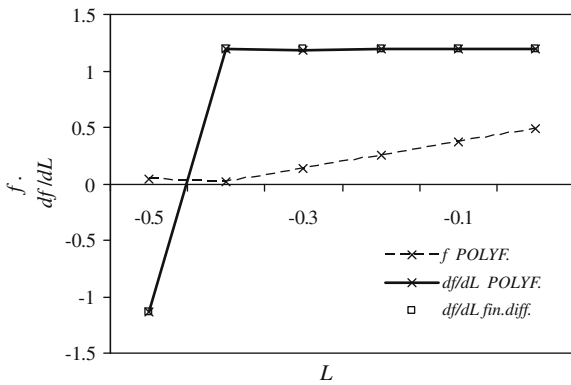


Fig. 19. Problem 5: performance measure f and sensitivity values df/dL for different values of the design variable L .

velocity with a constraint on the pressure drop, or vice versa. Looking at the values of f , we observe a very shallow local minimum for $L \approx -0.35$. This will cause some difficulties in obtaining a solution,

when starting from a design variable value close to 0.0, because the optimiser might then try to extend the parallel section to reduce the average tangential velocity. The sensitivity values of f , \bar{F}_1 and \bar{F}_2 , with respect to L are shown in Fig. 16, where we observe good agreement between the results obtained with FDM and the ones computed using the proposed procedure. We note that df/dL approaches zero for $L \approx -0.35$ which corresponds to a local minimum, while it attains a constant value for increasing L coincident with the constant slope of the asymptote to f . Table 6 contains the values of F_1 , F_2 and their sensitivities calculated with the solver and by finite difference. Fig. 17 finally depicts the FE configurations obtained for different values of L : $L = 0$, $L = 0.5$ and $L = 5$.

Problem 5. Design of the parallel section diameter with free surface height as performance measure.

Once the flow material leaves the die, significant deformation of the extrudate can be observed right after the die lip. We consider here that the material flows through the air at the die outlet. The aim of this example is to change the parallel zone height in order to obtain a given final extrudate, as shown in Fig. 18.

This problem has been modelled as an axisymmetrical flow with a free surface at the die outlet.

As design variable, we consider the parallel section height L shown in Fig. 18, subjected to the following constraints:

$$-0.45 \leq L \leq 1.0 \tag{41}$$

whereas the performance measure is defined in terms of the final height of the extrudate as

$$F = (G_{cal} - G_{imp})^2 \tag{42}$$

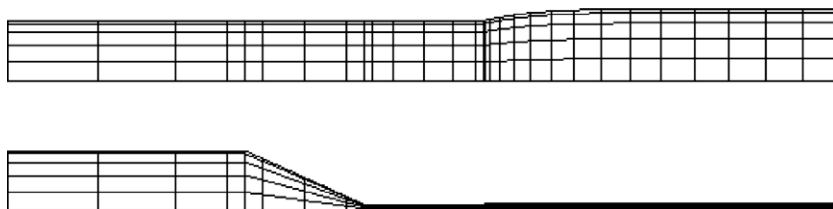


Fig. 20. Problem 5: FE discretization for different configurations: original configuration, $L = 0.0$ (top), and shrunk configuration, $L = -0.45$ (bottom).

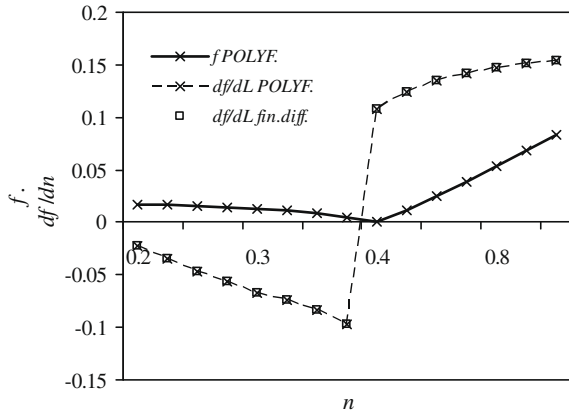


Fig. 23. Problem 6: performance measure f and sensitivity values df/dn for different design parameters n .

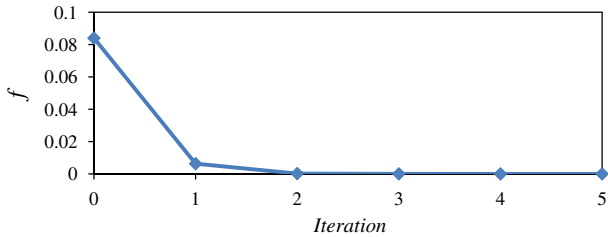


Fig. 24. Convergence history for Problem 6.

with G_{imp} the target extrudate height and G_{cal} the current free surface height calculated by the FE analysis.

The computed values of the performance measure and of its sensitivity are plotted in Fig. 19 for different values of L where we note that at $L \approx -0.414$ the performance function reaches a global minimum with $df/dL \approx 0$. For greater values of L , the sensitivity attains a constant value of around 0.189. Fig. 19 also displays the

sensitivity values obtained by using FDM which show a good agreement with those obtained with the proposed procedure. The convergence history of the optimization procedure is displayed in Fig. 20. Convergence occurred with the sixth design after having carried out 26 function evaluations. The optimal design is obtained for the value of $L = -0.414$ when the deviation of the computed radius of the extrudate from the imposed radius $G_{imp} = 0.1$ is 1.8×10^{-5} ; reduced down from 0.492 for the initial design. Fig. 21 depicts the two FE meshes for L equal to 0.0 and -0.45 .

Problem 6. Material design with free surface height as performance measure.

The objective of this example is to change the viscosity of the fluid in such a way that the resulting extrudate has a given height. The model problem is described in Fig. 22 with a free surface at the die outlet [33]. The fluid is modelled using the Navier–Stokes equations with the viscosity defined by the Bird Carreau model [34]:

$$\eta(\dot{\gamma}) = \eta_{\infty} + (\eta_0 - \eta_{\infty})(1 + (\lambda\dot{\gamma})^2)^{\frac{n-1}{2}} \tag{43}$$

where n , η_{∞} , η_0 and λ are material parameters and $\dot{\gamma}$ represents the shear rate.

The power law index n is assumed as design variable subjected to the conditions

$$0.0 \leq n \leq 1.0 \tag{44}$$

where for $n = 1$ we have the Newtonian fluid with viscosity η_0 . We consider the same performance measure as in the last example given by

$$F = (G_{cal} - G_{imp})^2 \tag{45}$$

where now f is defined as function of n .

Fig. 23 displays the values of the performance measures and of its sensitivity for different values of n . A local minimum in the performance measure can be observed for $n \approx 0.4$ where df/dn is nearly zero. For $n > 0.4$, the values of the sensitivity approaches a constant value equal to 0.154, whereas for $n < 0.4$ the sensitivity of the extrudate decreases considerably. The values of the sensitivity obtained by using FDM agree quite well with those obtained by

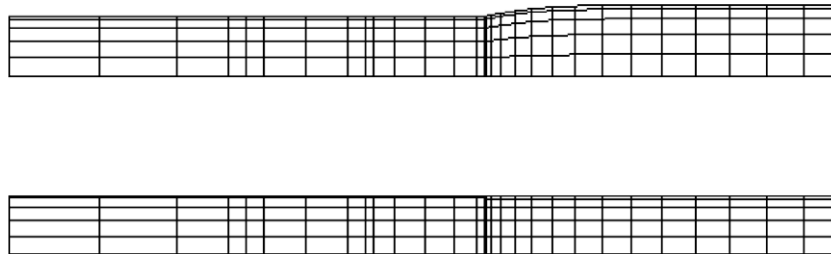


Fig. 25. Problem 6: FE meshes obtained for different value of the design variable n : for $n = 1.0$ (i.e. constant viscosity) (top) and for $n = 0.15$ (bottom).

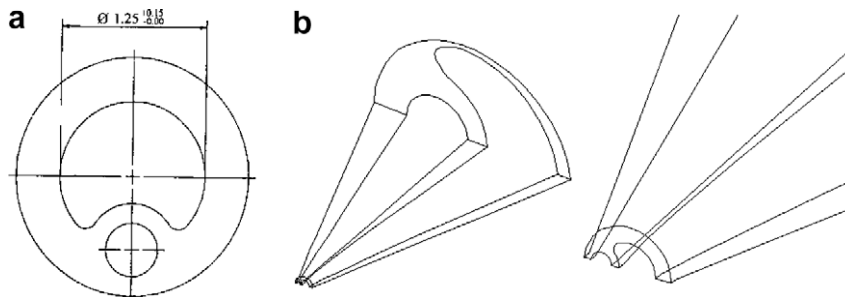


Fig. 26. Extrusion die design for the catheter. Exit geometry (a), IGES model of the conic section (b).

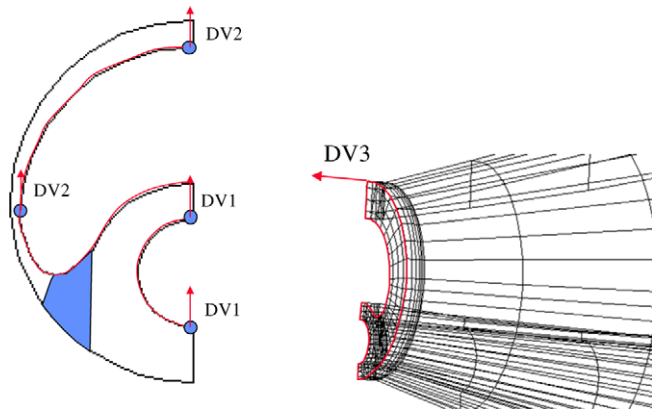


Fig. 27. Design variables for the catheter die.

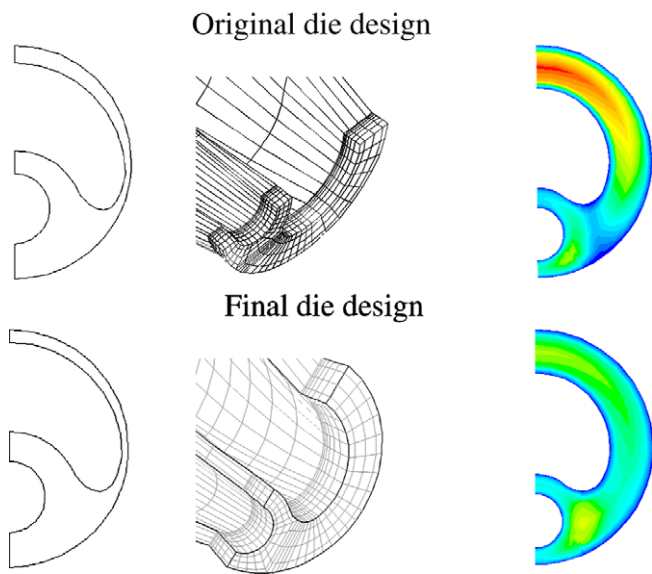


Fig. 28. Original and final (optimized) dies: inlet geometry (left), die land (center), exit velocity contour plots (right).

the proposed procedure as shown in the same Fig. 23. We can also observe that the performance measure seems to have a ‘kink’ which leads to a near vertical line in the gradient of the function. Nevertheless the functions are sufficiently smooth and they can be used for optimization with gradient-based methods without any major problems. The convergence of the optimization procedure

is shown in Fig. 24 where convergence occurred with the fifth design after 21 function evaluations. The optimal design is obtained for a value of $n = 0.393$ when the deviation of the computed radius of the extrudate from the imposed radius of $G_{imp} = 0.51$ is 4.86×10^{-6} ; reduced down from 0.084 for the initial design. The two FE meshes for n equal to 1.0 and 0.15 are plotted in Fig. 25.

The successful optimization of Problem 6 shows that it is possible to obtain a better working die by adjusting material parameters. However, for this example no attention was paid to whether it is possible to change the properties of the polymer used for the extrusion of this rod over such a large range using normal additives and/or by adjusting the temperature of the melt. Nevertheless, the variation of n is a useful die design criterion to adopt, for it can also be caused by changes in the raw material, processing conditions and/or performance of the die [35–38].

6. Industrial case studies

Typically, a traditional die design sequence involves the following steps,

Design → *Manufacture* → *Experimental balancing*

complemented by some flow simulations. The numerical procedure proposed in this paper allows us to change this die sequence into the following one:

Design → *Numerical balancing* → *Redesign* → *Manufacture* → *Experimental balancing*

Manufacture’s costs and experimental balancing steps are consequently drastically reduced with respect to traditional die design processes [39].

In this section we validate the procedure by solving two industrial case studies: a *catheter extrusion die* and a *rubber (flat profile) extrusion die*. Despite the sensitivities are calculated using the proposed procedure, no sensitivity results are shown hereafter, this is because the focus of this example is on the optimal industrial design of these dies.

Problem 7. Catheter extrusion die.

Objective of this application is to refine (or redesign) the initial die design shown in Fig. 26. The basic idea is that the die entry zone must be designed in such a way that the proper amount of melt enters both the upper and the lower parts of the die including a flow separator, and that the exit section must have the appropriate length. The fluid is modelled using the Navier–Stokes equations with the viscosity defined by

$$\eta(\dot{\gamma}) = \eta_0 \dot{\gamma}^{n-1} \tag{46}$$

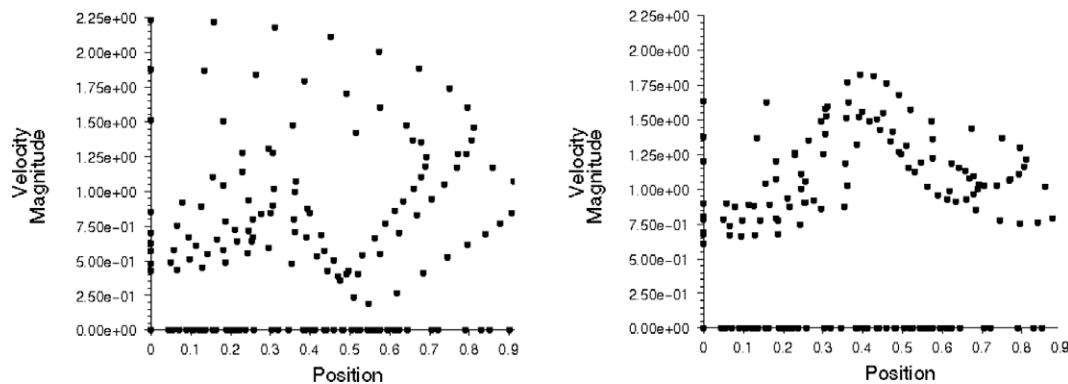


Fig. 29. Nodal velocity distribution over the exit area.

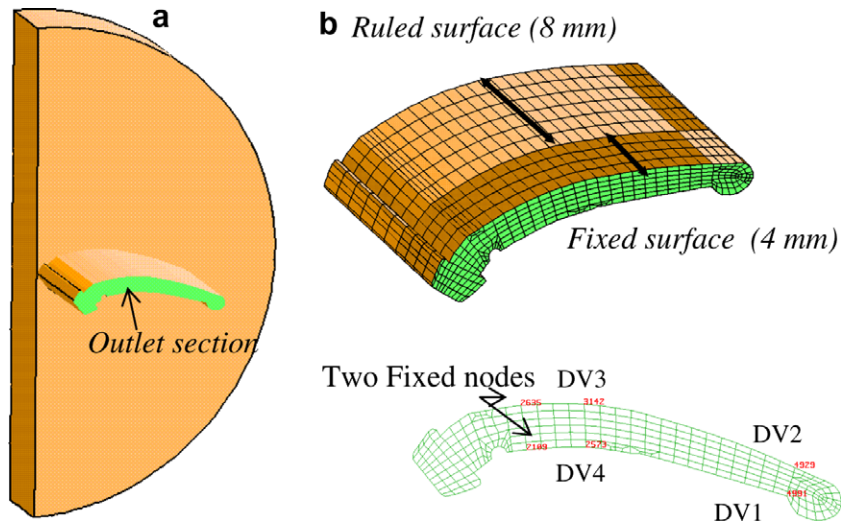


Fig. 30. Flat rubber profile die for optimization: flow domain (a), design variables and re-meshing sections (b).

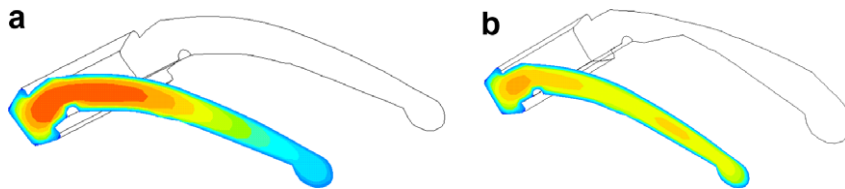


Fig. 31. Exit velocity profiles for parallel die (a) and die optimized using conical widening/narrowing (b).

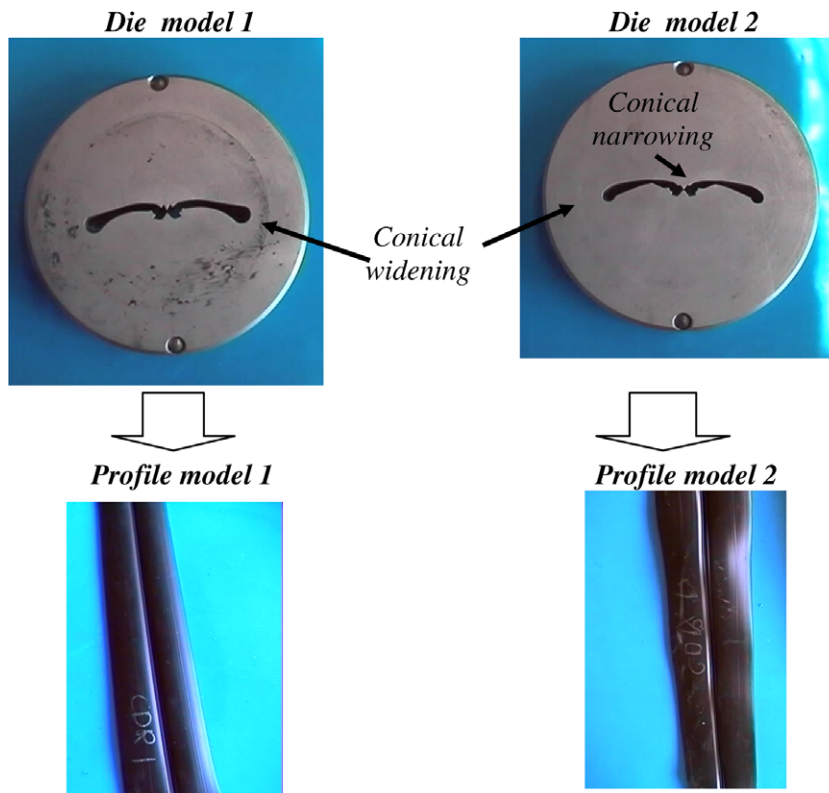


Fig. 32. Manufactured die exit plates for flat profile optimized using conical/narrowing.



Fig. 33. Profile cross-section.

where $n = 0.42$ and $\eta_0 = 1$ are the material parameters values. A volumetric flow rate of $1 \text{ mm}^3/\text{s}$ is considered in the simulations with zero velocity along the walls.

The aim is to achieve a uniform velocity profile distribution at the local die exit. By selecting the three design variables of Fig. 27, i.e. two at the entry and one that is the length of the parallel section at the die exit, the performance measure to be minimized is then defined as follows

$$F(dv_1, dv_2, dv_3) = \int_A v_z^2 dA \quad (47)$$

where v_z is the local velocity and A the cross section area. The constraints on the design variables are (in mm):

$$\begin{aligned} -0.1 &\leq dv_1 \leq 1.5 \\ -2.0 &\leq dv_2 \leq 1.0 \\ -2.0 &\leq dv_3 \leq 0.0 \end{aligned} \quad (48)$$

with the initial values of $(0.0, 0.0, -1.0)$. The optimized values of the design variables are $(0.237892, -0.0882171, -0.567113)$, with $F = 1.18531$, which have been obtained after 30 evaluations. The initial and optimized die designs are depicted in Fig. 28 together with the velocity distribution contours. The velocity contours along the exit section of the initial design show non-uniformity, evidencing that a strong imbalance of the flow would occur in any fully developed flow. The optimized die design, on the other hand, shows a significant improvement. This is confirmed in Fig. 29, where the spread of exit velocities is reduced from $[0.25 \text{ m/s}, 2.25 \text{ m/s}]$ down to $[0.6 \text{ m/s}, 1.9 \text{ m/s}]$.

Problem 8. Flat profile.

A rubber die is here designed as in Problem 7, by balancing the flow velocities at the exit. A power law for viscosity with zero velocity along the walls is also assumed here. The FE model of the flow domain of both, the die and the conical reservoir sections, are displayed in Fig. 30.

The displacement of the nodes shown in Fig. 30(b) are chosen as design variables, with an initial depth of 5 mm, and upper and lower bounds for the design variables of 5.0 mm and -1.0 mm, respectively. Two nodes on the cross section are assumed fixed. The optimization process will result in conical widening/narrowing, which can be achieved by defining a re-meshing zone by means of a ruled surface, as shown in Fig. 30(b).

Assuming the integral of the difference between the local and average velocities over the exit section as the performance measure, we can write:

$$F(dv_1, dv_2, dv_3, dv_4) = \int_A (v_z - \bar{v}_z)^2 dA \quad (49)$$

The velocity distribution is calculated for both the parallel die and the die balanced by conical widening/narrowing, which is displayed in Fig. 31.

To validate the optimization processes, two optimized die designs were manufactured. The profiles are depicted in Fig. 32. These samples have been designed by assuming different design

variables ranges. The manufactured profile obtained with the die design 2 is not straight showing some waviness all along its length whereas the profile manufactured with die design 1 shows a straight appearance. The final cross section of the profile is depicted in Fig. 33.

7. Conclusions

The growing emphasis on the design and optimization of manufacturing processes introduces new demands and challenges to industries. In order to make efficient the design of manufacturing processes, in this paper we have presented a numerical procedure for calculating the sensitivity and performance values which can be easily included within an existing FE code.

By reformulating the governing equations, the evaluation of the derivatives needed for the sensitivity analysis are obtained by a post-processing step of the iterative method used to solve the governing equations. The changes required in the code are hence kept to a minimum. Shape variations are evaluated using the domain parameterization method, whereas the direct differentiation method is used to solve the implicit variations of the state variables. Since the sensitivity formulations have been developed for the discretized system of equations, its accuracy will depend on the FE approximation.

Two analytical examples have been developed in detail to verify the proposed procedure, showing good agreement with the finite difference method and recovering the analytical solutions exactly. Numerical simulation and sensitivity analysis are combined to analyse three die design extrusion problems, with the melt flow modelled by the Navier–Stokes equations. The procedure is finally validated by the design optimization of two industrial applications, a catheter extrusion die and a rubber flat profile extrusion die.

In summary it has been shown that:

- The procedure allows one to perform the sensitivity analysis of the problem at hand by simply enlarging the system of equations that is sent to the solver.
- The sensitivity values are very accurate as long as we are dealing with accurate FE approximations.
- Time calculation is significantly saved as once the equilibrium equations are solved, the sensitivity of f can be calculated by simply performing a back substitution in Eq. (12).
- Excellent results are obtained when using the calculated sensitivity values in an optimization process.
- The procedure shows great versatility since a wide range of problems have been successfully solved.

Acknowledgements

The Swansea authors wish to acknowledge the support of the Welsh Assembly Government for the Knowledge Transfer Centre (KTC) “Welsh Composites Centre” funded out of the A4B programme. The authors also wish to thank VYGON, France, for the kind permission to publish the results from the optimization of the catheter extrusion die and HUTCHINSON, France, for the kind permission to publish the results from the optimization of the rubber dies.

Appendix A

In the isoparametric formulation of the FE method [40], the position variable x and the displacement field u are defined by the following mappings of the fixed reference domain $\xi \in [-1, 1]$:

$$\mathbf{x}(\xi) = \mathbf{N}(\xi)\mathbf{x}^e; \quad u(\xi) = N(\xi)\mathbf{u}^e \quad (50)$$

In Eq. (50), $\mathbf{x}^e = [x_1^e, x_2^e]$ and $\mathbf{u}^e = [u_1^e, u_2^e]$ denote the position and displacement of nodes 1 and 2, respectively, and $\mathbf{N} = [N_1, N_2]$ the shape functions defined as

$$N_1 = \frac{1 - \xi}{2}, \quad N_2 = \frac{1 + \xi}{2} \quad (51)$$

The corresponding elemental stiffness matrix and force vector, written in terms of the fixed reference domain, are then given as follows

$$\mathbf{K}^e(x) = K \int_{-1}^1 N_{,\xi}^T N_{,\xi} J_e^{-2} |J_e| d\xi, \quad \mathbf{C}^e(x) = \int_{-1}^1 \mathbf{N} |J_e| dx \quad (52)$$

where $N_{,\xi}$ denotes the derivative of N with respect to ξ and $J_e = \frac{dx}{d\xi} = \frac{L}{2N} = |J_e|$ is the Jacobian of the transformation from the reference coordinates ξ to the global coordinates. Note that \mathbf{K}^e and \mathbf{C}^e depend on x through J_e . From Eq. (52), it follows

$$\frac{\partial \mathbf{K}^e}{\partial \mathbf{x}} = - \sum_{n=1}^N K \int_{-1}^1 N_{,\xi}^T N_{,\xi} J_e^{-2} J_{e,x} d\xi \quad (53)$$

where we note that the shape design variations are represented by variations of the nodal coordinates, with the shape functions held fixed [17].

A.1. FE matrices for Problem 1

By accounting of Eqs. (51) and (52), the element stiffness matrix and force vector read as

$$\mathbf{K}^e = \frac{K}{(x_2^e - x_1^e)} \begin{bmatrix} 1 & -1 \\ -1 & 1 \end{bmatrix}, \quad \mathbf{C}^e = (x_2^e - x_1^e) \begin{bmatrix} \frac{1}{2} \\ \frac{1}{2} \end{bmatrix} \quad (54)$$

which yield the following residual vector

$$\mathbf{R}_{U}^e = \mathbf{K}^e \begin{Bmatrix} u_1^e \\ u_2^e \end{Bmatrix} - \mathbf{C}^e = - \begin{bmatrix} \frac{K}{(x_2^e - x_1^e)} (u_2^e - u_1^e) + \frac{(x_2^e - x_1^e)}{2} \\ \frac{K}{(x_2^e - x_1^e)} (u_1^e - u_2^e) + \frac{(x_2^e - x_1^e)}{2} \end{bmatrix} \quad (55)$$

The expression $(\frac{\partial \mathbf{R}_U}{\partial \mathbf{x}})^e$ at the element level is hence given as follows

$$\left(\frac{\partial \mathbf{R}_U}{\partial \mathbf{x}} \right)^e = \begin{bmatrix} \frac{K}{(x_2^e - x_1^e)^2} (u_1^e - u_2^e) + \frac{1}{2} \frac{K}{(x_2^e - x_1^e)^2} (u_2^e - u_1^e) - \frac{1}{2} \\ \frac{K}{(x_2^e - x_1^e)^2} (u_2^e - u_1^e) + \frac{1}{2} \frac{K}{(x_2^e - x_1^e)^2} (u_1^e - u_2^e) - \frac{1}{2} \end{bmatrix} \quad (56)$$

For Problem 1, where we use a mesh of equally spaced nodes, boundary conditions $u_1 = u_5 = 0$, and two design variables $[L, K]$, the global matrices employed in the Newton–Raphson procedure read as follows

$$\frac{\partial \mathbf{R}_U}{\partial \mathbf{u}} = \begin{bmatrix} \frac{2KN}{L} & \frac{-KN}{L} & 0 \\ \frac{-KN}{L} & \frac{2KN}{L} & \frac{-KN}{L} \\ 0 & \frac{-KN}{L} & \frac{2KN}{L} \end{bmatrix} \quad (57)$$

$$\frac{\partial \mathbf{R}_U}{\partial \mathbf{x}} = \begin{bmatrix} -\frac{KN^2}{L^2} u_3 & \frac{KN^2}{L^2} (u_3 - u_2) - \frac{1}{2} & 0 \\ \frac{KN^2}{L^2} (u_3 - u_2) + \frac{1}{2} & \frac{KN^2}{L^2} (u_2 - u_4) & \frac{KN^2}{L^2} (u_4 - u_3) - \frac{1}{2} \\ 0 & \frac{KN^2}{L^2} (u_4 - u_3) + \frac{1}{2} & \frac{KN^2}{L^2} u_3 \end{bmatrix} \quad (58)$$

$$\left(\frac{\partial \mathbf{R}_U}{\partial L} \right)^e = 0, \quad \left(\frac{\partial \mathbf{R}_U}{\partial K} \right)^e = \frac{(u_2^e - u_1^e)}{x_2^e - x_1^e} \begin{bmatrix} -1 \\ 1 \end{bmatrix} \quad (59)$$

$$\frac{\partial \mathbf{R}_U}{\partial \mathbf{b}} = \begin{bmatrix} \frac{\partial R_U}{\partial L} & \frac{\partial R_U}{\partial K} \end{bmatrix} = \begin{bmatrix} 0 & \frac{N}{L} (2u_2 - u_3) \\ 0 & \frac{N}{L} (2u_3 - u_2 - u_4) \\ 0 & \frac{N}{L} (2u_4 - u_3) \end{bmatrix} \quad (60)$$

$$\frac{\partial \mathbf{R}_X}{\partial L} = \begin{bmatrix} \frac{\partial R_{X_2}}{\partial L} \\ \frac{\partial R_{X_3}}{\partial L} \\ \frac{\partial R_{X_4}}{\partial L} \end{bmatrix} = \begin{bmatrix} -\frac{1}{N} \\ -\frac{2}{N} \\ -\frac{3}{N} \end{bmatrix} \quad (61)$$

$$\frac{\partial R_F}{\partial \mathbf{u}} = \begin{bmatrix} \frac{\partial R_F}{\partial u_2} & \frac{\partial R_F}{\partial u_3} & \frac{\partial R_F}{\partial u_4} \end{bmatrix} = [0 \quad -2(u_3 - 1) \quad 0] \quad (62)$$

with the global residual given by

$$\mathbf{R} = \begin{bmatrix} R_L \\ R_K \\ R_{X_2} \\ R_{X_3} \\ R_{X_4} \\ R_{U_2} \\ R_{U_3} \\ R_{U_4} \\ R_F \\ R_G \end{bmatrix} = \begin{bmatrix} -\frac{L}{N} - \frac{KN}{L} (u_3 - 2u_2) \\ -\frac{L}{N} - \frac{KN}{L} (u_2 - 2u_3 + u_4) \\ -\frac{L}{N} - \frac{KN}{L} (u_3 - 2u_4) \\ x_2 - \frac{L}{N} \\ x_3 - \frac{2L}{N} \\ x_4 - \frac{3L}{N} \\ f - (u_3 - 1)^2 \\ g - L + 2 \\ L - \bar{L} \\ K - \bar{K} \end{bmatrix} \quad (63)$$

References

- [1] Fissler L. Entwicklung von Software-Tools zur Unterstützung der Auslegung von Profil-Extrusionswerkzeugen. Diplomarbeit, Gebr. Kötter GmbH, Abt. T-WZK, Pirmasens, Germany.
- [2] Laporte E, Le Tallec P. Numerical methods in sensitivity analysis and shape optimization. Boston: Birkhäuser; 2003.
- [3] Tiller MM. Sensitivity analysis and optimization of enclosure radiation with applications to crystal growth. PhD thesis, University of Illinois, Urbana-Champaign, USA, 1995.
- [4] Haslinger M, Dantzig. Implementation of design sensitivity analysis and numerical optimization in engineering analysis. Appl Math Modell 1996;20:792–9.
- [5] Haslinger J, Mäkinen RAE. Introduction to shape optimization: theory, approximation, and computation. Philadelphia: SIAM; 2003.
- [6] Choi KK, Kim N-H. Structural sensitivity analysis and optimization. 1: Linear systems. New York: Springer; 2005.
- [7] Choi KK, Kim N-H. Structural sensitivity analysis and optimization. 2: Non-linear systems and applications. New York: Springer; 2005.
- [8] Haftka RT, Gürdal Z, Kamat MP. Elements of structural optimization. Dordrecht: Kluwer Academic Publishers; 1990.
- [9] Tortorelli DA, Michaleris P. Design sensitivity analysis: overview and review. Inverse Probl Eng 1994;1:71–105.
- [10] Balagandhar D, Roy S. Design sensitivity analysis and optimization of steady fluid-thermal systems. Comput Methods Appl Mech Eng 2001;190:5465–79.
- [11] Balagandhar D, Tortorelli DA. Design of large-deformation steady elastoplastic manufacturing processes. Part II: Sensitivity analysis and optimization. Int J Numer Methods Eng 2000;49:933–50.
- [12] Smith DE. Design sensitivity analysis and optimization for polymer sheet extrusion and mold filling processes. Int J Numer Methods Eng 2003;57:1381–411.
- [13] Smith DE, Tortorelli DA, Tucker III CL. Optimal design for polymer extrusion. Part I: Sensitivity analysis for nonlinear steady-state systems. Comput Methods Appl Mech Eng 1998;167:283–302.
- [14] Smith DE, Tortorelli DA, Tucker III CL. Optimal design for polymer extrusion. Part II: Sensitivity analysis for weakly coupled nonlinear steady-state systems. Comput Methods Appl Mech Eng 1998;167:302–23.
- [15] Srikanth A, Zabarar N. Shape optimization and perform design in metal forming processes. Comput Methods Appl Mech Eng 2000;190:1859–901.
- [16] Smith DE, Tortorelli DA, Tucker III CL. Analysis and sensitivity analysis for polymer injection and compression molding. Comput Methods Appl Mech Eng 1998;167:325–44.
- [17] Vidal CA, Lee HS, Haber RB. The consistent tangent operator for design sensitivity analysis of history dependent response. Comput Syst Eng 1992;2(5–6):509–23.
- [18] Phelan DG, Haber RB. Sensitivity analysis of linear elastic systems using domain parametrization and mixed mutual energy principle. Comput Methods Appl Mech Eng 1989;77:31–59.
- [19] Cardoso JB, Arora JS. Variational method for design sensitivity analysis in nonlinear structural mechanics. AIAA J 1988;26:595–603.
- [20] Haug EJ, Choi KK, Komkov V. Design sensitivity analysis of structural systems mathematics in science and engineering. Orlando, FL: Academic Press; 1986 [1996].
- [21] Kim NH, Yi K, Choi KK. A material derivative approach in design sensitivity analysis of three-dimensional contact problems. Int J Solids Struct 2002;39:2087–108.
- [22] Vidal CA, Haber RB. Design sensitivity analysis for rate-independent elastoplasticity. Comput Methods Appl Mech Eng 1993;107:393–431.
- [23] Phelan DG, Vidal C, Haber RB. An adjoint variable method for sensitivity analysis of non-linear elastic systems. Int J Numer Methods Eng 1991;31:1649–67.
- [24] POLYFLOW, <<http://www.polyflow.be>>.
- [25] Brabant V, Fleury C. Shape optimal design and CAD oriented formulation. Eng Comput 1986;1:193–204.
- [26] DOT, <<http://www.vrand.com/DOT.html>>.

- [27] Sienz J, Silva CEK, Hinton E. Computer aided design of profile extrusion dies. In: Papadarakakis M, Topping BHV, editors. Innovative computational methods for structural mechanics. Stirlingshire, UK: Saxe-Coburg Publications; 1999. p. 271–303 (Chapter 13).
- [28] Produktkatalog 1997, Gebr. Kömmerling GmbH, 1997.
- [29] Sienz J, Szarvasy I, Pittman JFT, Hinton E, Sander R. Computer aided simulation and design of profile extrusion dies. Conf. of polymer processing, Europe/Africa Region Meeting 1997, Gothenburg, Sweden.
- [30] Svabik J., Mikulenka T, Manas M, Busby JW. Evaluation of profile die design strategies. Conf. of polymer processing, Europe/Africa Region Meeting 1997, Gothenburg, Sweden.
- [31] Carneiro OS, Nóbrega JM, Pinho FT, Oliveira PJ. Computer aided rheological design of extrusion dies for profiles. Mater Process Technol 2001;114:75–86.
- [32] Szarvasy I, Sienz J, Pittman JFT, Hinton E. Computer aided optimization of profile extrusion dies: definition and assessment of the objective function. Int Polym Process 2000;1:28–39.
- [33] Bathe KJ, Zhang H, Wang MH. Finite element analysis of incompressible and compressible fluid flows with free surfaces and structural interactions. Comput Struct 1995;56:193–213.
- [34] Bird RB, Armstrong RC, Hassager O. Dynamics of polymeric liquids. Fluid mechanics, vol. 1. New York: Wiley; 1987.
- [35] Bates SJ, Pittman JFT, Sienz J, Langley DS. Enhancing slit die performance by optimization of restrictor profiles. Polym Eng Sci 2003;43:1500–11.
- [36] Sienz J, Bates SJ, Pittman JFT. Flow restrictor design for extrusion slit dies for a range of materials: simulation and comparison of optimization techniques. Finite Elem Anal Des 2006;42:430–53.
- [37] Bates SJ. Development of robust simulation, design and optimization techniques for engineering applications. PhD Thesis, School of Engineering, Swansea University, Swansea, UK, 2003.
- [38] Bates SJ, Sienz J, Pittman JFT, Langley DS. Application of robust design optimisation to extrusion slit die design. In: Proceedings of the 3rd international conference on engineering computational technology, 2002, Prague.
- [39] Ettinger HJ, Sienz J, Pittman JFT. Parameterization and optimization strategies for the automated design of uPVC profile extrusion dies. Struct Multidiscip Optimiz 2004;28:180–94.
- [40] Bathe KJ. Finite element procedures. Englewood Cliffs, NJ: Prentice-Hall; 1982.